https://doi.org/10.5194/egusphere-2026-2215
Preprint. Discussion started: 12 May 2026

Frequent occurrence of newly formed aerosol particles over wide geographical areas in the Arctic free troposphere and atmospheric boundary layer

David J. Simon[1], Jonas Schaefer[1], Jörg Hartmann[2], Benjamin Kirbus[3], Joshua Müller[3], Markus Hartmann[1], Bruno Wetzel[1], Laura Köhler[2], Anna-Marie Jörss[2], Kay Weinhold[1], Andreas Herber[2], Zsófia Jurányi[2], Silvia Henning[1], Gregory C. Roberts[4], Manfred Wendisch[3], Mira L. Pöhlker[1,3], and Frank Stratmann[1]

[1]Atmospheric Microphysics Department, Leibniz Institute for Tropospheric Research, Leipzig, Germany
[2]Alfred Wegener Institute, Helmholtz Centre for Polar and Marine Research, Bremerhaven, Germany
[3]Leipzig Institute for Meteorology, Leipzig University, Leipzig, Germany
[4]Scripps Institution of Oceanography, La Jolla, CA, USA

Correspondence: David J. Simon (simon@tropos.de)

Abstract. New particle formation (NPF) can impact the Arctic radiative energy budget since this region is particularly sensitive to changes in aerosol particle and cloud condensation nuclei concentrations. Prior studies have predominantly investigated NPF in the Arctic atmospheric boundary layer (ABL), concluding that this phenomenon primarily takes place close to the surface. However, this study shows that NPF may take place throughout the entire lower Arctic troposphere. We have reached this conclusion by analyzing particle number size distribution data collected during a springtime aircraft campaign in the vicinity of Svalbard, the Fram Strait, and northern Greenland. We detected newly formed aerosol particles at various altitudes ranging from about 60 m to 3900 m and identified three atmospheric scenarios for their occurrence: newly formed particles in the free troposphere, in the ABL over sea ice, and in the vicinity of clouds. Our results suggest that regional Arctic atmospheric processes as well as long-range transport play key roles in the formation of new particles. Based on our data, we furthermore conclude that NPF may be a frequent and geographically extended phenomenon in the Arctic free troposphere.

1 Introduction

Aerosol particles are an important component of the global climate system (Forster et al., 2021). They enter the atmosphere either directly by primary emissions or are formed in situ by secondary aerosol particle formation from condensable gases (Seinfeld and Pandis, 2006). The latter process, which generates particles with diameters of initially a few nanometers, is termed new particle formation (NPF) (Kulmala et al., 2004). Depending on the atmospheric thermodynamic conditions, subsequent growth can increase particle sizes to values large enough such that the particles may act as cloud condensation nuclei (CCN) (Kulmala and Kerminen, 2008; Kerminen et al., 2018). CCN play a crucial role in cloud formation, affecting cloud life time, precipitation formation, and cloud albedo, thereby influencing Earth's radiative energy budget (Andreae and Rosenfeld, 2008; Forster et al., 2021). Globally, about 50 % of CCN are estimated to result from NPF (Gordon et al., 2017; Pierce and Adams,

https://doi.org/10.5194/egusphere-2026-2215
Preprint. Discussion started: 12 May 2026

2009; Merikanto et al., 2009). In the Arctic, with commonly low background aerosol particle number concentrations, NPF is particularly important because of the high susceptibility of Arctic cloud formation (and hence cloud radiative forcing) to changes in aerosol particle and CCN number concentrations under low aerosol levels (Mauritsen et al., 2011; Leaitch et al., 2013; Carslaw et al., 2013; Gordon et al., 2017).

Currently, the Arctic is changing rapidly in response to global climate change (Box et al., 2019; Wendisch et al., 2017, 2023). Among others, these changes manifest in a substantial decrease of the Arctic sea ice cover, especially at the end of the Arctic summer in September (Stroeve et al., 2007). Furthermore, an increase of the near-surface air temperature is observed, which exceeds the global average warming by a factor of two to three (Wendisch et al., 2023). The processes causing the intensified response of the Arctic climate system to global climate change are commonly referred to as Arctic amplification (Serreze and Francis, 2006; Serreze and Barry, 2011; Wendisch et al., 2023). A changing Arctic also entails consequences for the Arctic aerosol population. For example, the decline of the sea ice cover affects both primary emissions from the ocean surface and secondary formation of aerosol particles (Willis et al., 2018; Schmale et al., 2021). Concerning the latter, enhanced emissions of precursor gases from open sea surfaces, leads, or through thinning sea ice have been reported and are expected to proceed as the sea ice fractures and retreats further (Cuevas et al., 2018; Galí et al., 2019). There is direct evidence reported by Dall'Osto et al. (2017, 2018) who found a correlation between an increase of NPF events and decreasing sea ice extent. Furthermore, altered meridional transport may lead to enhanced aerosol particle and/or precursor transport into the Arctic, for instance, via warm-air intrusions (Dada et al., 2022; Wendisch et al., 2023, 2024), which are expected to occur more frequently in the future (Bintanja et al., 2020; Wendisch et al., 2025).

NPF has been observed in several locations Arctic-wide (Willis et al., 2018; Schmale and Baccarini, 2021). Most studies were based on measurements conducted during shipborne campaigns or at ground-based stations including Alert, Villum, Zeppelin, Tiksi, and Utqiagvik (e.g., Leaitch et al., 2013; Allan et al., 2015; Croft et al., 2016; Asmi et al., 2016; Freud et al., 2017; Baccarini et al., 2020; Beck et al., 2021). These stations provide temporally extended datasets and enable the analysis of annual cycles and long-term trends. Yet, inherently, station- and ship-based measurements can hardly provide precise vertical information. However, data on the vertical distribution of NPF are crucial to identify and study key transport and formation processes, and ultimately, to assess the corresponding effects on the Arctic climate (Lee et al., 2019; Schmale et al., 2021; Price et al., 2023). There are remote sensing instruments such as lidar that can provide vertical information on aerosol particles, but these methods mostly miss the required sensitivity to reliably infer quantitative information on NPF. Consequently, to observe and analyze NPF, airborne measurements with balloons, helicopters, or aircraft appear indispensable (Garrett et al., 2002; Weber et al., 2003; Engvall et al., 2008; Kupiszewski et al., 2013; Willis et al., 2016, 2017; Burkart et al., 2017; Pilz et al., 2024). These latter airborne studies predominantly suggested that NPF close to the surface inside the atmospheric boundary layer (ABL) prevails, and that free tropospheric NPF is less common (Willis et al., 2018).

In this paper, rather than focusing on the process of NPF itself (i.e., the initial nucleation mechanism), we investigate the occurrence of newly formed particles produced by NPF, which have initial diameters of less than 20 nm (Kulmala et al., 2004). Here, we report on the frequent occurrence of these newly formed particles at various altitudes ranging from about 60 m to 3900 m above sea level. The corresponding data were collected during an aircraft campaign carried out in the Fram Strait,

https://doi.org/10.5194/egusphere-2026-2215
Preprint. Discussion started: 12 May 2026

surrounding the Svalbard Archipelago, and in the vicinity of Villum Research Station (Station Nord) in Greenland in April 2024. Our data show that newly formed particles can be found throughout the entire lower Arctic troposphere, which indicates that both local processes and long-range transport are important causes for NPF in the Arctic.

2 Methods

2.1 Aircraft campaign overview

The airborne campaign "Boundary layer and Aerosol and Cloud Study in the Arctic, based on aircraft and T-Bird Measurements II" (BACSAM II) was conducted from 5 April to 2 May 2024. We carried out eleven research flights (RFs) with the German research aircraft Polar 6 (P6, Wesche et al., 2016), operated by the Alfred Wegener Institute, Helmholtz Centre for Polar and Marine Research (AWI; see supporting information (SI) Fig. S1 for a map of all flight paths). With the operational base in Longyearbyen (Svalbard), target areas included the Fram Strait, the Svalbard Archipelago, and the vicinity of Villum Research Station in north-eastern Greenland. Flights were conducted between 7 and 29 April 2024. This time period was characterized by persistent warm air advection driven by low pressure systems south-west of Svalbard, resulting in above-average surface temperatures in Svalbard. Two exceptions with typical cold conditions and high pressure at the beginning of the campaign from 7 to 11 April and from 15 to 17 April occurred. Note that our sampling is potentially biased towards viable flight conditions, i.e., high visibility at Longyearbyen Airport. Furthermore, we preferred cloud-free conditions in the target regions or elevated cloud layers (cloud base $\gtrapprox 200\,\mathrm{m}$), and no precipitation.

2.2 Aerosol measurements and detection of newly formed particles

Aboard the P6 aircraft, we measured aerosol particle number size distributions (PNSDs) with a mobility particle size spectrometer (MPSS, Wiedensohler et al., 2012, 2018). The custom-built MPSS measures the PNSDs in the particle diameter size range between 10 nm and 850 nm based on the electric mobility of aerosol particles with a time resolution of about 300 s. In this paper, we only use data up to 600 nm since on some measurement days arcing inside the differential mobility analyzer (DMA) led to artifacts in the PNSDs appearing at larger diameters. The system features a Vienna-type DMA (built by the Leibniz-Institute for Tropospheric Research) and a condensation particle counter (CPC, TSI model 3760A, TSI Incorporated, USA). For further details on the MPSS system see Wiedensohler et al. (2012, 2018). The flow in the sampling tubing leading to the MPSS was manually adjusted depending on the true airspeed of the aircraft (typically $\approx 60\ \mathrm{ms}^{-1}$ during legs in the target area and $\approx 90\ \mathrm{ms}^{-1}$ during transit flights) to achieve near-isokinetic sampling. As the onboard-temperature was significantly higher than the ambient temperature, the relative humidity of the sampled air in the aerosol inlet was below 40 %. Consequently, all reported particle diameters refer to dry conditions (Jurányi et al., 2025). All particle number concentration data have been corrected to standard conditions (1013 hPa and 273.15 K).

In this paper, we distinguish between NPF and newly formed particles. Since the minimum diameter of aerosol particles that can be detected with our measurement instrumentation is 10 nm, it is not feasible to clearly identify the exact region where

https://doi.org/10.5194/egusphere-2026-2215
Preprint. Discussion started: 12 May 2026

NPF occurred, i.e., where the process of the initial nucleation of particles with sizes of about 2 to 3 nm from condensable gases took place (Kulmala et al., 2004; Kerminen et al., 2018). Nevertheless, particle sizes of 10 nm still imply that these particles were newly formed by secondary particle formation (i.e., by NPF, Kulmala et al., 2004). We hence refer to these particles as newly formed particles. To detect newly formed particles, we fitted mono-modal, bi-modal, or tri-modal log-normal functions to the MPSS-measured PNSDs, with the different modes representing nucleation, Aitken, and accumulation modes, respectively. Following Kulmala et al. (2004), we refer to aerosol particles in the measured dry diameter range from below 10 nm to 20 nm as nucleation mode particles, from 20 nm to 90 nm as Aitken mode particles, and from 90 nm to 600 nm as accumulation mode particles. We consider an MPSS-measured PNSD as indicative for newly formed particles if the fitted distribution features a nucleation mode with a geometric mean diameter below 10 nm. See Sect. S2.1 for further details and examples of fitted PNSDs, indicating either the presence or absence of newly formed particles (Fig. S2). Only distributions measured at a constant altitude were considered for quantitative analysis, i.e., PNSDs measured during the aircraft's ascents and descents were not taken into account in quantitative terms.

2.3 Meteorological measurements

A nose boom was installed at the tip of the aircraft to measure air pressure, temperature, and the three-dimensional wind vector. The nose boom features an Aventech five-hole probe to measure static, dynamic, and differential pressures to derive the wind vector from these data, and an open-wire Pt100 in an unheated Rosemount housing to record air temperature data. These data were measured with a time resolution of 100 Hz. Humidity data are available at 20 Hz from a Vaisala HMT333 in a Rosemount housing installed aboard the aircraft. Position and altitude were measured by combining Global Positioning System (GPS) and Inertial Navigation System (INS) data, which were recorded at 100 Hz. See Hartmann et al. (2018) for further details on the instrumentation and data processing.

2.4 Backwards trajectory analysis

Backward trajectories were calculated from ERA5 wind fields (Hersbach et al., 2020) utilizing the Lagrangian analysis tool LAGRANTO (Sprenger and Wernli, 2015). The trajectories were initiated every minute along the flight track of the P6 at the corresponding flight altitude. The trajectories were calculated for 120 hours backwards in one minute time steps and several meteorological parameters from ERA5 were traced along the trajectory. Based on these parameters, we carry out an analysis of air mass history in Sect. 3. Among others, we determine the last contact of these air masses with clouds based on the specific cloud liquid water content ($CLWC$) and the specific cloud ice water content ($CIWC$). Here, we consider an air mass to have been in contact with a cloud if $CIWC > 0.01\,\mathrm{g\,kg^{-1}}$ or $CLWC > 0.1\,\mathrm{g\,kg^{-1}}$.

https://doi.org/10.5194/egusphere-2026-2215
Preprint. Discussion started: 12 May 2026

3 Results and discussion

3.1 Frequent occurrence of newly formed particles

Throughout the entire BACSAM II campaign, we frequently observed newly formed particles over large areas of the Arctic region studied (Fig. 1). Newly formed particles were detected during all eleven research flights, with the first observation of such particles on 7 April 2024, and the last on 29 April 2024. We encountered newly formed particles at various locations (approximately between 76°N to 85°N and 15°W to 26°E) and altitudes ranging from about 60 m to 3900 m above sea level (Fig. 1). The time periods during which we identified newly formed particles amount to an overall duration of about 10 hours and 30 minutes, which corresponds to approximately 24 % of the total flight time of all research flights and a distance flown of about 2800 km.

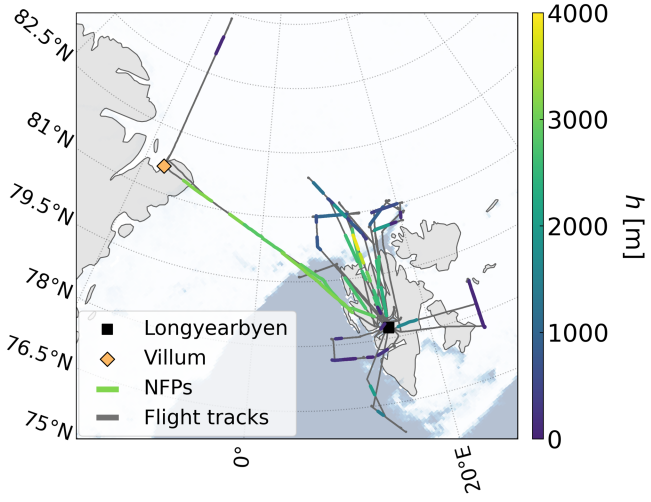

Figure 1. Geographical location and altitude at which newly formed particles (NFPs) were observed during the BACSAM II campaign. The flight tracks are shown in gray and the locations where newly formed particles were identified are color-coded by the corresponding flight altitude. The sea ice concentration is shown exemplary for 15 April 2024, during which we encountered newly formed particles at low altitudes over the ice-covered sea east of Svalbard (see Sect. 3.3). The corresponding sea ice data were retrieved from www.seaice.uni-bremen.de (Spreen et al., 2008).

We categorize the observations according to three distinct environmental conditions (Fig. 2). These include newly formed particles in the free troposphere (without clouds being present, Sect. 3.2), newly formed particles at low altitudes in the ABL over sea ice (Sect. 3.3), and newly formed particles in the vicinity of clouds (Sect. 3.4). The reader is referred to Fig. S3 for the median size distributions of the PNSDs indicating the presence of newly formed particles, for each of the three environments. Furthermore, we report the related temperature and relative humidity conditions prevailing during observations of newly formed particles in Sect. S3 and Fig. S4.

Newly formed particles detected in the free troposphere account for the majority of our observations with about 45 % of all

https://doi.org/10.5194/egusphere-2026-2215
Preprint. Discussion started: 12 May 2026

cases (i.e., 45 % of all PNSDs featuring newly formed particles), compared to about 16 % in the ABL over sea ice, and approximately 25 % in the vicinity of clouds (Fig. 2a). About 14 % of all observations cannot clearly be assigned to one of the categories (Sect. S2.2). Newly formed particles were frequently detected in a wide range of altitudes between approximately 60 m and 3900 m (Fig. 2b, c). Here, 60 m and 3900 m correspond to the minimum and maximum flight altitudes at which measurements were carried out. Consequently, we cannot rule out that newly formed particles could be present at altitudes even higher than 3900 m. In Fig. 2c, we show the relative frequency of occurrence of newly formed particles per altitude, defined as the duration of newly formed particle-observations per altitude, normalized by the total time of all PNSD measurements within this altitude bin. The frequency values show a rather uniform vertical distribution from the surface up to about 2000 m, with roughly 25 % of all measured PNSDs featuring newly formed particles. At altitudes between about 2500 m and 3200 m, where measurements were overwhelmingly carried out in the cloud-free free troposphere (Fig. 2b), newly formed particles were detected more frequently, with up to 67 % of PNSDs measured at these altitudes indicating the presence of newly formed particles (Fig. 2c).

To additionally provide a general overview of particle number concentrations prevailing throughout the campaign, Fig. 2d presents the median vertical distribution of particle number concentrations in the total measurement size range from 10 nm to 600 nm and in the nucleation mode size range from 10 nm to 20 nm, calculated from the data available from all flights. The values span roughly two orders of magnitude, with nucleation mode particles, e.g., contributing between 50 % to 75 % of all measured particles at altitudes of about 1000 m and 3000 m.

Note that during the campaign, sampling times and consequently number of PNSDs measured, as well as distances flown at certain altitudes, were not evenly distributed over the investigated altitudes, geographical locations, and synoptic conditions. For example, while measurements in the lowest 100 m were carried out for a total duration of approximately 390 min (over a distance of about 1480 km), measurements at 3500-3600 m and 3800-3900 m were solely performed during one research flight, and at each altitude range for merely 5 to 10 min (27 to 54 km, to feature one full MPSS scan; hatched bars in Fig. 2c). The values of duration and relative frequency of newly formed particle-occurrence reported in this section are thus not intended to constitute representative values for the lower Arctic troposphere, but rather represent statistics of the observations made during the BACSAM II campaign.

Nevertheless, our measurements clearly demonstrate that newly formed particles can frequently be found throughout the lower Arctic troposphere and, as these particles originate from secondary particle formation, suggest that NPF in the Arctic occurs across large geographical areas and over a wide range of altitudes. In this context, it is worth noting that no indications for the presence of newly formed particles were found within or near the cloud-free ABL over open ocean (Sect. S2.2).

To further elucidate the atmospheric scenarios under which newly formed particles were observed, and to gain insights into potential precursor gases and their origins, in the following sections, the results of case studies focusing on newly formed particles in the free troposphere, inside the ABL over sea ice, and in the vicinity of clouds will be presented. First, specific examples for these three scenarios will be given. Second, to put the given examples into a larger perspective, we will discuss respective backward trajectory analyses for all air masses featuring newly formed particles for each of the three environments.

https://doi.org/10.5194/egusphere-2026-2215
Preprint. Discussion started: 12 May 2026

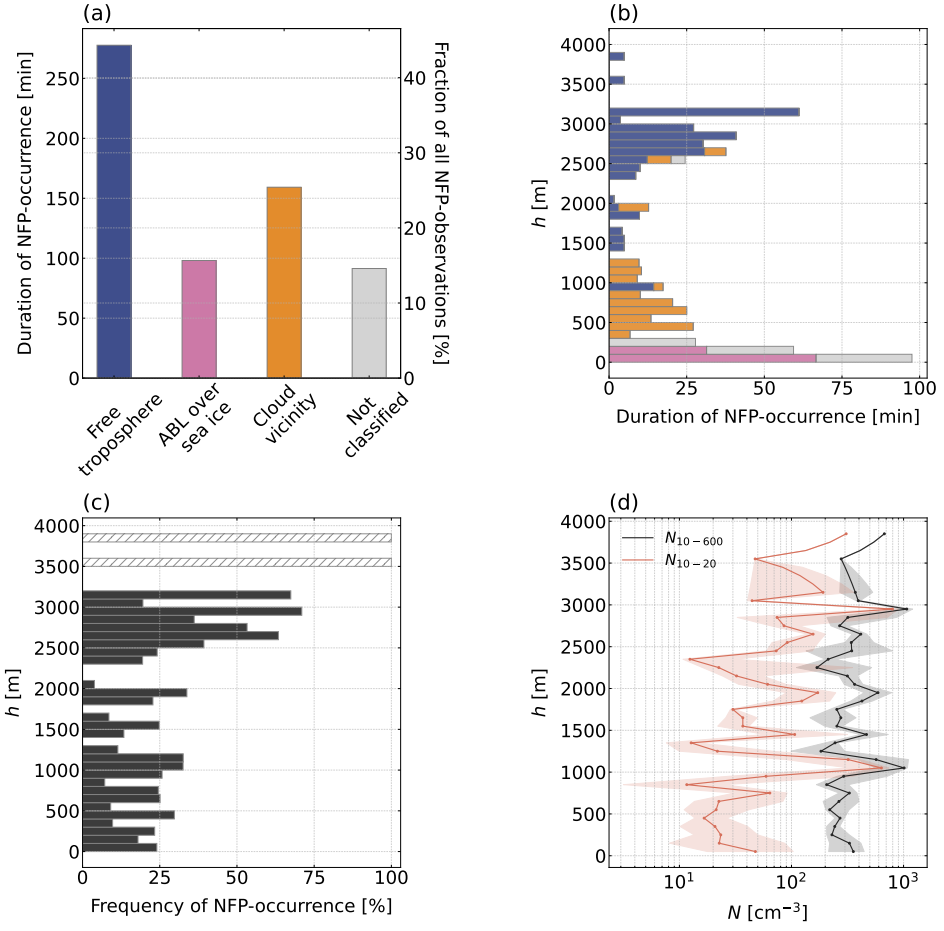

Figure 2. **(a)** Duration of newly formed particle-occurrence (NFP-occurrence) for each of the categories, which are introduced in detail in the main text (left y-axis). Ratio of NFP-observations per category to all NFP-observations combined (right y-axis). **(b)** Duration of NFP-occurrence per measurement altitude, grouped into height bins with a width of 100 m. The data are shown as stacked bars. **(c)** Relative frequency of NFP-occurrence per measurement altitude, grouped into height bins with a width of 100 m. The hatched bars at altitudes higher than 3500 m indicate that here only one full PNSD measurement was conducted within each altitude bin. **(d)** Median values (solid lines) and interquartile ranges (shaded area) of integral particle number concentrations in the total measured size range ($10\ \mathrm{nm} \leq D_\mathrm{p} \leq 600\ \mathrm{nm}$) and in the nucleation mode size range ($10\ \mathrm{nm} \leq D_\mathrm{p} \leq 20\ \mathrm{nm}$), respectively.

https://doi.org/10.5194/egusphere-2026-2215
Preprint. Discussion started: 12 May 2026

3.2 Newly formed particles in the free troposphere

Here, as an illustrative example, we present results concerning newly formed particles in the free troposphere which were encountered on 13 April 2024 during RF04 while transiting from Longyearbyen (Svalbard) to Villum Research Station (northern Greenland) at an altitude of 2890 m (Fig. 3a).

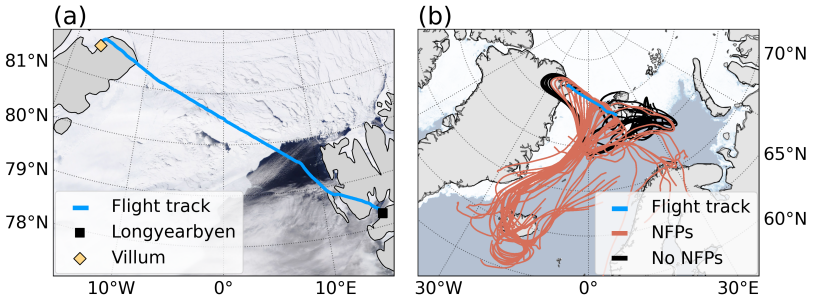

Figure 3. (a) Flight track of RF04 on 13 April 2024. The Moderate-resolution Imaging Spectroradiometer (MODIS)-TERRA satellite image was retrieved from https://wvs.earthdata.nasa.gov. **(b)** Five-day backward trajectories along the flight track. Backward trajectories associated with newly formed particles (NFPs) are depicted in red and backward trajectories connected to PNSD measurements featuring no newly formed particles in black. The sea ice concentration data were retrieved from www.seaice.uni-bremen.de (Spreen et al., 2008).

In the two days ahead of the flight, a low pressure system located over the east coast of Greenland advected warm and moist air over the sea ice edge in the Fram Strait (red trajectories in Fig. 3b). Within this warm-air intrusion, North Atlantic ABL air was lifted up to the free troposphere. The uplifting over the sea ice edge was accompanied with the formation of precipitating clouds, which dissipated before sampling of the air mass. Consequently, the sampled free tropospheric air was cloud-free. The cumulus clouds visible in the satellite image in Fig. 3a capped the marine ABL, which was located more than 2 km beneath the flight track. Therefore, we expect no influence of these low-level clouds on our measurements in the free troposphere. In addition to the southerly air masses from the Atlantic, air masses originating at higher latitudes close to Svalbard were probed during RF04 (black trajectories in Fig. 3b).

During the time period from about 6:23 to 7:40 UTC, flying at high altitudes (≈ 2890 m), and covering a distance of about 409 km, we encountered elevated number concentrations in the lower MPSS size bins (Fig. 4). Detected particle number concentrations in the size range from 10 nm to 20 nm reached on average values of about $N_{10-20} \approx 714\ \mathrm{cm}^{-3}$, which constituted about 66 % of the total particle number concentration measured in the range from 10 nm to 600 nm (Fig. 4c). The measured PNSDs featured a sharp decline in the size range from 10 nm to about 60 nm, i.e., we observed the "upper" end of a pronounced nucleation mode (see Fig. S5 for the related median PNSD). In other words, we detected newly formed particles in the Arctic free troposphere across a large geographical area.

For the time period 7:40 to 8:19 UTC, encountered PNSDs featured no distinct nucleation mode, and number concentrations in the size range from 10 nm to 20 nm were substantially lower ($N_{10-20} \approx 25\ \mathrm{cm}^{-3}$, 16 % of the total MPSS-measured number concentration, Fig. 4c), i.e., no or only a small number of newly formed particles were present.

https://doi.org/10.5194/egusphere-2026-2215
Preprint. Discussion started: 12 May 2026

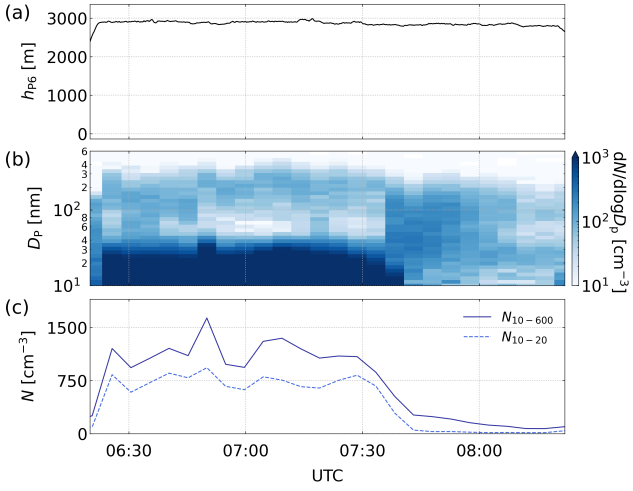

Figure 4. **(a)** P6 altitude during RF04 on 13 April 2024. **(b)** MPSS-measured PNSD. **(c)** Integral particle number concentrations in the total measured size range ($10\ \mathrm{nm} \leq D_\mathrm{p} \leq 600\ \mathrm{nm}$, solid line) and in the nucleation mode size range ($10\ \mathrm{nm} \leq D_\mathrm{p} \leq 20\ \mathrm{nm}$, dashed line), respectively.

Notably, the newly formed particles were associated with air masses originating from lower latitudes which were transported into the Arctic within a warm-air intrusion (red trajectories in Fig. 3b), while for the northerly air masses no newly formed particles were detected (black trajectories in Fig. 3b).

The presence of newly formed particles in the Arctic free troposphere distinguishes our observations from previous airborne studies utilizing aircraft and helicopter measurements, which pointed towards NPF within the ABL as the dominant source of newly formed particles in the Arctic (Engvall et al., 2008; Kupiszewski et al., 2013; Burkart et al., 2017; Willis et al., 2016, 2017). Together with a number of ground-based studies highlighting the importance of NPF within the ABL (e.g., Ström et al., 2009; Leaitch et al., 2013; Freud et al., 2017; Croft et al., 2016; Dall'Osto et al., 2017, 2020; Baccarini et al., 2020; Beck et al., 2021), these results led researchers to assume that NPF in the Arctic primarily occurs close to the surface (e.g., Willis et al., 2018; Dall'Osto et al., 2017, 2020). However, high numbers of newly formed particles in the Arctic free troposphere have occasionally been reported before (Wiedensohler et al., 1996; Weber et al., 2003). For example, Weber et al. (2003) conducted systematic aircraft measurements in the free troposphere of the Canadian Arctic from January to May 2000. During one of 38 research flights, they observed one clear NPF event at an altitude of approximately 4200 m. During the other 37 flights of their campaign, no indications for NPF occurring at high altitudes were found. Analyzing measurements conducted with a tethered balloon system, Pilz et al. (2024) reported enhanced number concentrations of aerosol particles in the size range from 12 nm to 150 nm concurrently with low concentrations of particles larger than 150 nm in the summertime Central Arctic during the Multidisciplinary drifting Observatory for the Study of Arctic Climate (MOSAiC) expedition. The authors hypothesized that NPF taking place aloft lead to these elevated concentrations of smaller particles but were unable to constrain potential sources and associated processes due to a limited maximum measurement altitude of 1000 m and because of missing PNSD

https://doi.org/10.5194/egusphere-2026-2215
Preprint. Discussion started: 12 May 2026

measurements. Our data support these latter observational results and indicate that NPF might occur frequently in the Arctic free troposphere over large geographical areas.

Backward trajectory analysis of all air masses featuring newly formed particles in the free troposphere

To further elucidate free tropospheric newly formed particles, which we observed on eight different days, considering all research flights performed during BACSAM II, and utilizing backward trajectories, a systematic analysis of free tropospheric air mass history was carried out. We investigated both free tropospheric air masses that show clear signs of newly formed particles, and free tropospheric air masses that exhibit no indications of newly formed particles. Every minute of each flight, we initiated a five-day backward trajectory at the pressure altitude of the aircraft. Hence, the air sampled during one PNSD measurement, which lasts for approximately 5 minutes and indicates either the presence or absence of newly formed particles, is represented by five backward trajectories. The results of the analysis are presented in Fig. 5, which depicts median values of meteorological and geographical parameters along the trajectories of all flight sections carried out in the free troposphere throughout the campaign.

Predominantly, air masses featuring newly formed particles in the free troposphere originated further south compared to air masses with no indications for free tropospheric newly formed particles, and gradually moved poleward at high altitudes during the five days prior to arrival (Fig. 5a-c). Initially, these air masses connected to newly formed particle were warmer and contained more moisture (Fig. 5d, f). About 60 hours before arrival, temperatures of air masses linked to newly formed particles started to decrease, and between 24 to 48 hours prior to arrival, specific humidities decreased as well. The latter might be caused by the formation of (precipitating) clouds, as already mentioned in the case study above. Consequently, air masses associated with newly formed particles became colder and less humid compared to air masses showing no signs of free tropospheric newly formed particles. Generally, about 80 % of all backward trajectories linked to free tropospheric newly formed particles were influenced by clouds on their way to the measurement location (Fig. 5i). In contrast, only 28 % of the backward trajectories featuring no newly formed particles were in contact with a cloud during the last five days before arrival (Fig. 5i). Higher values of northward integrated water vapor transport (IVT_{north}), most notably during the last 12 to 48 hours, show that in the whole column more water vapor was transported poleward for cases when newly formed particles were observed in the Arctic free troposphere (Fig. 5g). None of the backward trajectories featuring newly formed particles resided in the ABL for the last 12 hours prior to arrival at the track of the P6, and less than 2 % of these trajectories passed through the ABL in the last 54 hours. About 71 % of the backward trajectories had no contact with the ABL for the last five days (Fig. 5h).

These findings suggest that newly formed particles in the Arctic free troposphere are connected to poleward transport of warm and moist air, as occurring, e.g., during warm-air intrusions (Wendisch et al., 2024). Furthermore, because the trajectories overwhelmingly remained in the free troposphere during the transport to the measurement region, the results indicate that the precursor gases involved in the formation of these particles originated from long-range transport from lower latitudes, with NPF very likely occurring in the Arctic free troposphere. Such a transport pathway for precursor gases resulting in free tropospheric NPF has already been suggested in a modeling study by Price et al. (2023). Furthermore, the above findings imply

https://doi.org/10.5194/egusphere-2026-2215
Preprint. Discussion started: 12 May 2026

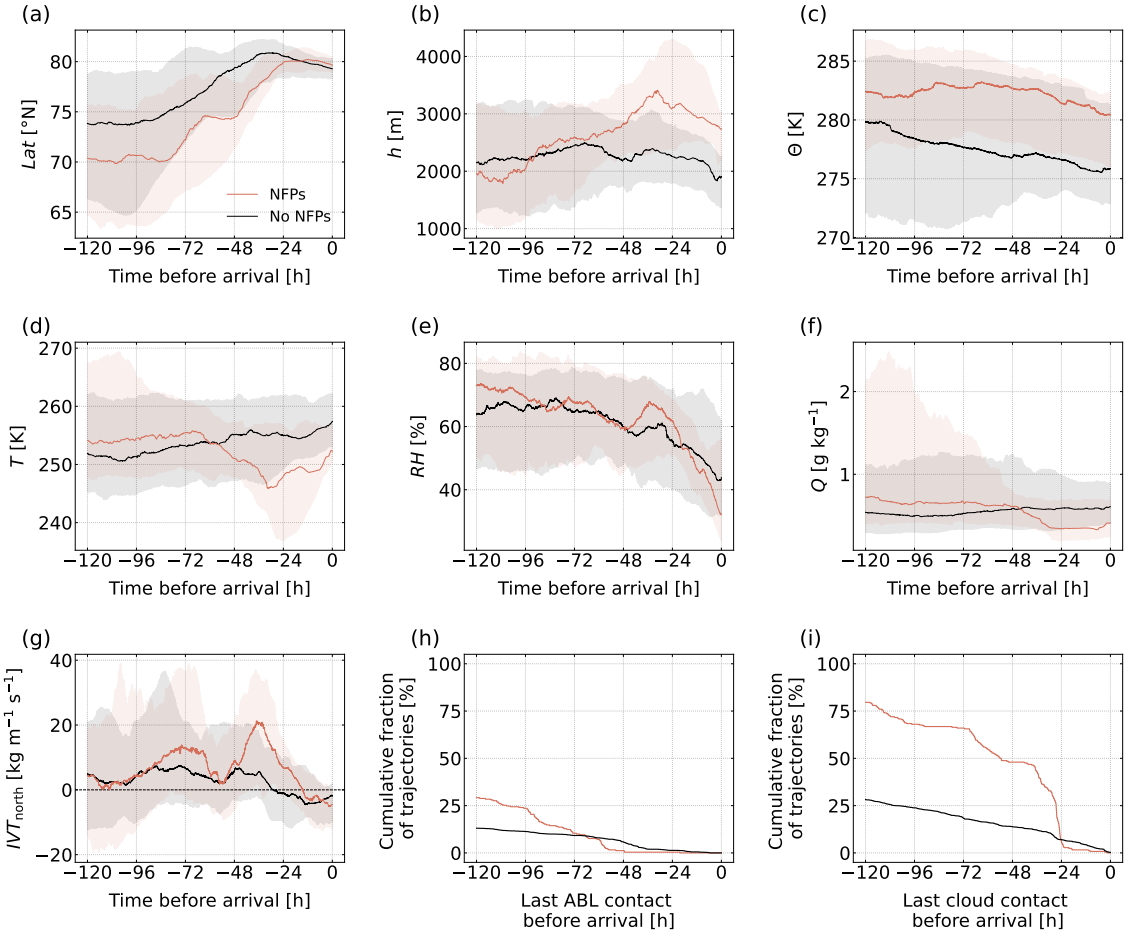

Figure 5. Comparison of geographical and meteorological parameters along the backward trajectories of flight sections in the free troposphere between trajectories connected to the presence (red) and absence (black) of newly formed particles (NFPs). Shown, as a function of time prior to arrival at the measurement location, are median values (solid lines) and interquartile ranges (shaded areas) of **(a)** latitude Lat, **(b)** altitude h, **(c)** potential temperature Θ, **(d)** absolute temperature T, **(e)** relative humidity RH, **(f)** specific humidity Q, and **(g)** northward integrated water vapor transport IVT_{north}. The last two subplots show the cumulative fraction of the last contact of the trajectories with the **(h)** ABL and **(i)** clouds. Note that if the cumulative fraction does not increase to 100 % at $t = -120\,\mathrm{h}$, this indicates that a fraction of the trajectories was not in contact with the ABL/clouds during the last five days (the maximum time span the calculated trajectories cover).

a potential role for clouds in the transport and possibly transformation of precursors, e.g., through releasing precursor gases from evaporating cloud droplets (Weber et al., 2001; Wehner et al., 2015). Precipitation caused by these clouds might have also increased the probability for NPF to occur by removing large aerosol particles, thus decreasing the pre-existing surface area and consequently reducing scavenging of gaseous precursors and newly formed particles (Perry and Hobbs, 1994; Weber et al., 2001).

This leads us to the hypothesis that meridional transport in combination with cloud processing, occurring in connection with,

https://doi.org/10.5194/egusphere-2026-2215
Preprint. Discussion started: 12 May 2026

e.g., warm-air intrusions, may play an important role in Arctic NPF by delivering the ingredients (precursor gases including water vapor) to locations (high altitudes) with favorable conditions (intense solar radiation, low temperatures) for NPF.

3.3 Newly formed particles inside the atmospheric boundary layer over sea ice

Inside the ABL, newly formed particles were detected, e.g., on 15 April 2024 during RF05 while flying east of Svalbard at low altitudes (approximately 70 m and 155 m) over sea ice, where cracks as well as open and partly refrozen leads were present (see Fig. S6). The associated flight track is shown in Fig. 6a, with Fig. 6b depicting the backward trajectories for the air masses encountered along the flight track.

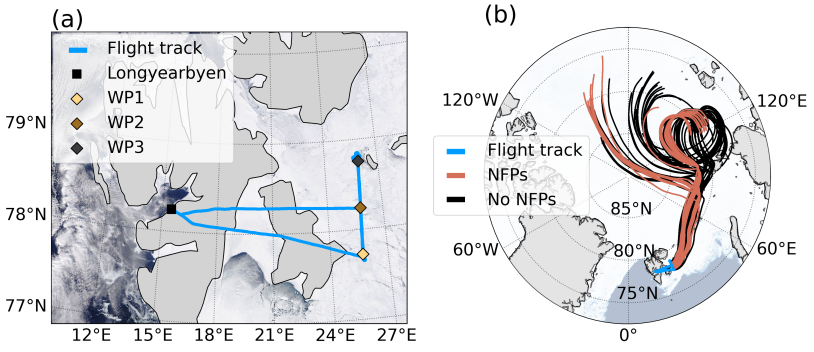

Figure 6. (a) Flight track of RF05 on 15 April 2024. The MODIS-TERRA satellite image was retrieved from https://wvs.earthdata.nasa.gov. **(b)** Five-day backward trajectories along the section of the flight track shown in Fig. 7. Backward trajectories associated with newly formed particles (NFPs) are depicted in red and backward trajectories connected to PNSD measurements featuring no newly formed particles in black. The sea ice concentration data were retrieved from www.seaice.uni-bremen.de (Spreen et al., 2008).

The area investigated was subject to the anti-cyclonic flow around a high pressure system north of Svalbard, causing cold air advection from the central Arctic to the target region. This meteorological situation resulted in air masses that exclusively originated in the high Arctic and traveled towards the P6 flight track from higher latitudes over sea ice-covered regions (Fig. 6b). All the way between waypoint 1 (WP1) and WP3, over a distance of about 115 km, clear sky conditions prevailed (Fig. 6a).

The presence of newly formed particles was indicated by elevated aerosol particle number concentrations in the lower size bins of the PNSDs, featuring a distinct nucleation mode, which we observed during three consecutive legs at altitudes of $\approx 70\,\mathrm{m}$ and $\approx 155\,\mathrm{m}$ between WP1 and WP3 (Fig. 7). Mean number concentrations in the nucleation mode size range reached $N_{10-20} \approx 191\ \mathrm{cm}^{-3}$ (time period 10:03 to 10:39 UTC), $N_{10-20} \approx 170\ \mathrm{cm}^{-3}$ (11:08 to 11:22 UTC), and $N_{10-20} \approx 114\ \mathrm{cm}^{-3}$ (12:17 to 12:40 UTC), accounting for about 39 %, 37 %, and 30 % of the total MPSS-measured aerosol particle number concentrations. In contrast, during the leg at $\approx 850\,\mathrm{m}$ altitude (11:30 to 12:00 UTC) between WP1 and WP3, as well as during the transit to and from the target region at $\approx 1360\,\mathrm{m}$ altitude, the PNSDs featured low number concentrations in the nucleation

https://doi.org/10.5194/egusphere-2026-2215
Preprint. Discussion started: 12 May 2026

mode size range (Fig. 7, $N_{10-20} \approx 3\ \mathrm{cm}^{-3}$, 1 % of the total MPSS-measured particle number concentration at 850 m). From the vertical profiles of potential temperature obtained during the ascents and descents at WP1, WP2, and WP3 (Fig. 7a), we determine an ABL height of about 170 m in the region of interest (see Fig. S7). Thus, the three legs at 70 m and 155 m, during which newly formed particles were detected, were carried out inside the ABL, while the leg at higher altitude ($\approx 850\,\mathrm{m}$), as well as the transits to and from the region of interest, took place in the free troposphere.

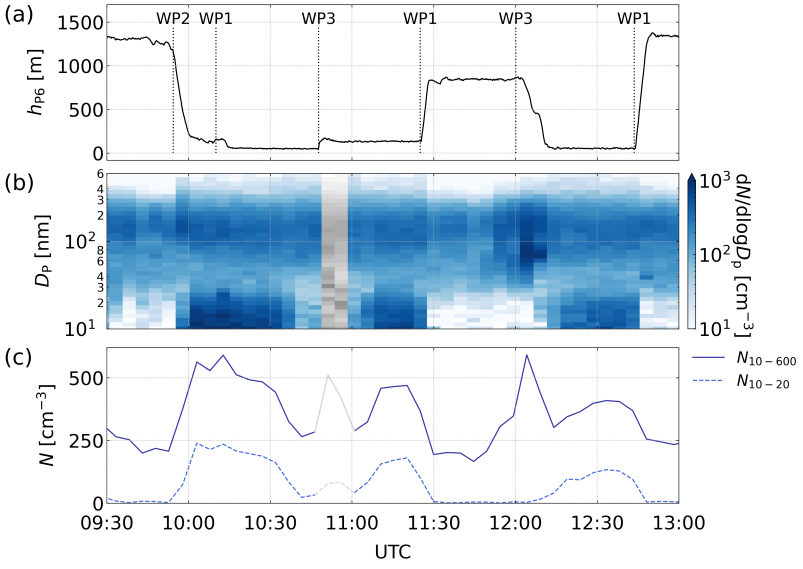

Figure 7. (a) P6 altitude during RF05 on 15 April 2024. **(b)** MPSS-measured PNSD. **(c)** Integral particle number concentrations in the total measured size range ($10\ \mathrm{nm} \leq D_\mathrm{p} \leq 600\ \mathrm{nm}$, solid line) and in the nucleation mode size range ($10\ \mathrm{nm} \leq D_\mathrm{p} \leq 20\ \mathrm{nm}$, dashed line), respectively. The data measured from 10:51 to 11:01 UTC are grayed out in panels (b) and (c) since erroneous measurements due to possible sampling of aircraft exhaust cannot be ruled out.

Integral aerosol particle number concentrations in the total measured size range (10 nm to 600 nm) and in the size range from 10 nm to 20 nm decreased from WP1 to WP3, i.e., from south to north (Fig. 6a, Fig. 7c). The spatial variability of the number concentration of nucleation mode particles suggests geographically heterogeneous processes and points toward newly formed particles as the result of regional formation rather than long-range transport, as the latter would likely lead to rather constant concentrations of newly formed particles along the flight track. Interestingly, the particle number concentrations in the nucleation mode size range from 10 nm to 20 nm recorded during the legs inside the ABL between WP1 and WP3 (i.e., in the same area) decreased not only spatially, but also over time (Fig. 7c). In addition to the integral values shown above, Fig. S8 depicts median PNSDs for each of the three legs close to the surface individually, which likewise shows that number concentrations of particles in the nucleation mode reduce over time. This temporal variability points toward a regional source as well, since it suggests that we observed an NPF event that becomes weaker throughout the day. However, we are not able to unambiguously resolve if the precursors involved in NPF originated directly from the sea ice-covered measurement region, with various cracks and leads being present (Fig. S6), or if the precursors were transported to the target area from the higher

https://doi.org/10.5194/egusphere-2026-2215
Preprint. Discussion started: 12 May 2026

Arctic. But, in our view, it appears feasible to conclude that the spatial and temporal variability of the newly formed particles encountered here (i.e., the decrease of sub-20 nm particles from WP1 to WP3 and throughout the day) and the similar origin of air masses featuring newly formed particles and air masses without newly formed particles (Fig. 6b) rather indicate a regional source.

In the Arctic, precursor gases reported to contribute to NPF and particle growth include dimethylsulfide (DMS, which oxidizes to methansulfonic acid (MSA) and sulfuric acid (SA)), ammonia, organics, and iodic acid (Willis et al., 2018; Schmale and Baccarini, 2021). The latter, in particular, has been linked to NPF in Arctic sea ice-covered regions (Allan et al., 2015; Sipilä et al., 2016; Baccarini et al., 2020; Beck et al., 2021). It has been shown for both the Arctic and Antarctica that iodine can be emitted from the sea ice. Potential sources include marine microalgae (diatoms) growing below the sea ice (Hill and Manley, 2009; Atkinson et al., 2012), where the iodine can be emitted through cracks and leads and has been connected to thinning Arctic sea ice (Cuevas et al., 2018). The sea ice itself or the snowpack can also release iodine via abiotic, photo-chemical processes (Gálvez et al., 2016; Kim et al., 2016; Raso et al., 2017). Yet, since we cannot resolve the particle composition of nucleation mode particles nor conducted gas-phase measurements, at this point, we cannot ultimately determine the precursor gases resulting in the newly formed particles observed in this case study. Nevertheless, these previous results suggest the sea ice-covered target area as a plausible source region of precursor gases and newly formed particles.

Backward trajectory analysis of all air masses featuring newly formed particles in the atmospheric boundary layer over sea ice

To further investigate the occurrence of newly formed particles inside the ABL over sea ice, an analysis of air mass history was carried out for the respective observations made during our campaign. Newly formed particles inside the ABL over sea ice were found twice, i.e., on 15 April (case study) and on 13 April for approximately 15 min north of Villum Research Station (see Fig. 1). Fig. 8 presents the results of the backward trajectory analysis carried out for both days.

Both days were characterized by cold air masses from northern latitudes which traveled over sea ice-covered regions (median sea ice concentration values between ≈ 93 % and 100 %, Fig. 8a, b, e). The air masses featured low specific humidities, but, due to cold temperatures, high relative humidities (w.r.t. water, Fig. 8e-g). Furthermore, the data suggest that all trajectories resided inside the ABL during the last 24 hours (Fig. 8i) before arriving at the P6, providing the possibility for precursor uptake. A difference between the two air mass histories is the time since the last cloud contact before arrival (Fig. 8j). The air masses encountered on 13 April (RF04) had no cloud contact for at least four days, while during RF05 on 15 April, last cloud contact of more than 50 % of the trajectories occurred about 24 h before arrival in the target region. For both days, the trajectories descended during the last five days. This decrease in altitude is more pronounced for the event on 15 April (Fig. 8c), with the lowest altitude along the trajectories reached just before arrival at the aircraft. The descent of the backward trajectories again indicates rather regional precursor sources as the gases are very likely emitted from the surface.

From these observations, we hypothesize that the observed presence of newly formed particles in the ABL over sea ice is connected to precursor gases (conceivably iodine components) which originate from natural, most likely regional, but possibly also higher-latitude Arctic sources within the sea ice, from leads, or snow.

https://doi.org/10.5194/egusphere-2026-2215
Preprint. Discussion started: 12 May 2026

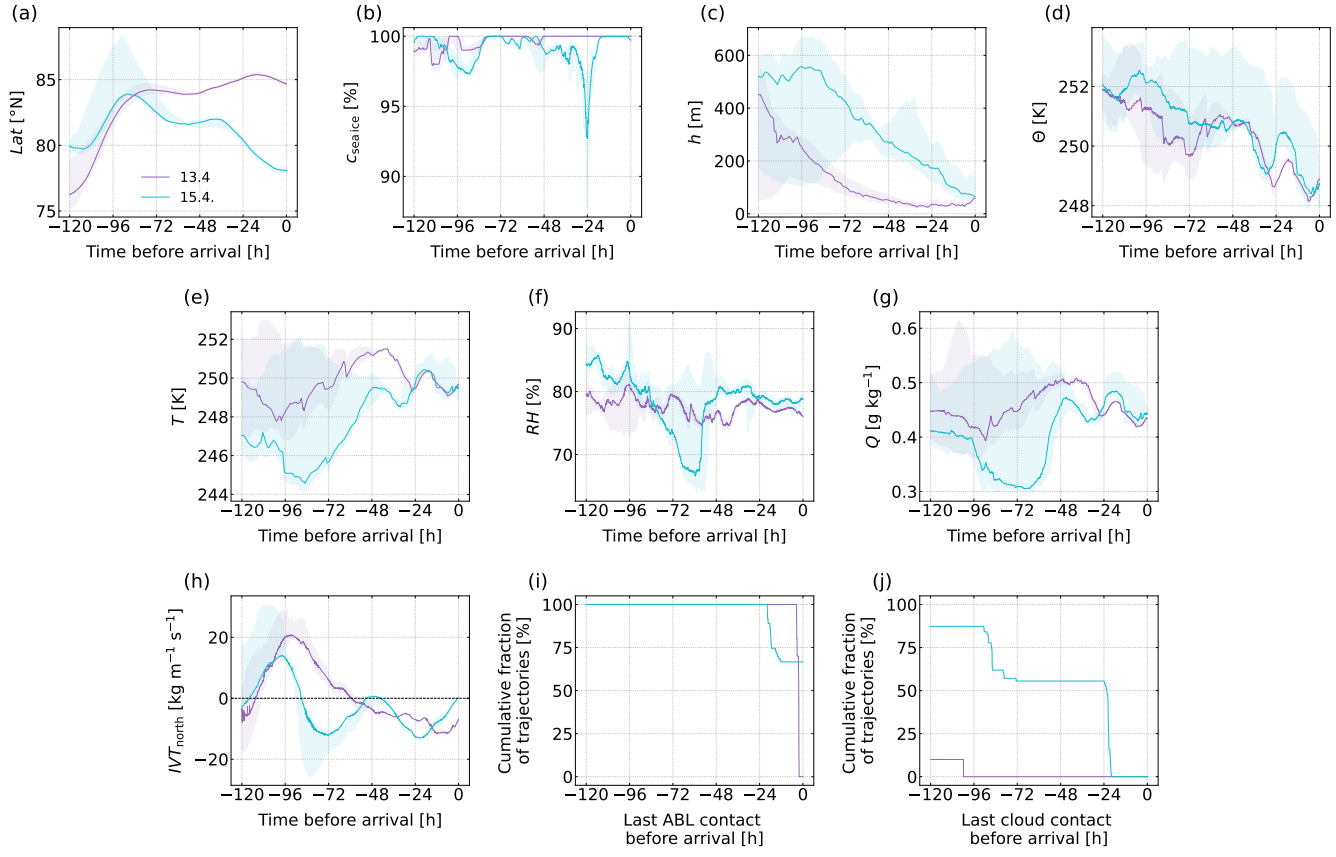

Figure 8. Comparison of geographical and meteorological parameters along the backward trajectories of flight sections linked to newly formed particles inside the ABL over sea ice for the events on 13 and 15 April. Shown, as a function of time prior to arrival, are median values (solid lines) and interquartile ranges (shaded areas) of **(a)** latitude Lat, **(b)** sea ice concentration c_{seaice}, **(c)** altitude h, **(d)** potential temperature Θ, **(e)** absolute temperature T, **(f)** relative humidity RH, **(g)** specific humidity Q, and **(h)** northward integrated water vapor transport IVT_{north}. The last two subplots show the cumulative fraction of the last contact of the trajectories with the **(i)** ABL and **(j)** clouds. Note that if the cumulative fraction does not increase to 100 % at $t = -120\,\text{h}$, this indicates that a fraction of the trajectories was not in contact with the ABL/clouds during the last five days (the maximum time span the calculated trajectories cover).

3.4 Newly formed particles in the vicinity of clouds

Newly formed particles in the vicinity of clouds were, e.g., encountered on 24 April 2024 during RF08, while flying north of Svalbard over sea ice (open leads and cracks were present, see Fig. S9) with an initially slightly broken and then closed stratocumulus cloud deck (Fig. 9a). Measurements were carried out below cloud base and at cloud top.

On 24 April, a high pressure system was centered directly over Svalbard, resulting in westerly flow in the target region. The air mass probed at altitudes between approximately 600 m and 1200 m originated either in the North Atlantic close to Greenland, near Iceland, or northern Scandinavia (red trajectories in Fig. 9b), and was advected from the North Atlantic marine ABL and

https://doi.org/10.5194/egusphere-2026-2215
Preprint. Discussion started: 12 May 2026

lifted above the sea ice, where this layer was decoupled from the surface (Sect. S6.2, Fig. S10). At the top of that elevated mixed layer, stratocumulus clouds were present (Fig. 9a), with a cloud base at about 800 m altitude, and cloud top at about 1150 m. The air mass that was probed at about 2100 m in the free troposphere originated in northern Canada and passed over Greenland on its way to the P6 position (black trajectories in Fig. 9b).

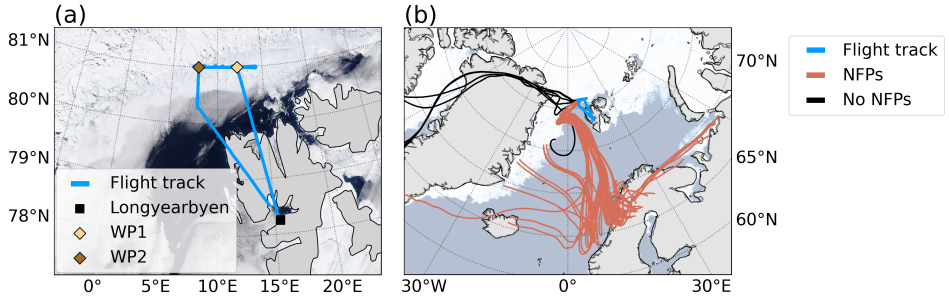

Figure 9. (a) Flight track of RF08 on 24 April 2024. The MODIS-TERRA satellite image was retrieved from https://wvs.earthdata.nasa.gov. **(b)** Five-day backward trajectories along the section of the flight track shown in Fig. 10. Backward trajectories associated with newly formed particles (NFPs) are depicted in red and backward trajectories connected to PNSD measurements featuring no newly formed particles in black. The sea ice concentration data were retrieved from www.seaice.uni-bremen.de (Spreen et al., 2008).

Here, we specifically discuss the data collected between WP1 and WP2 over a distance of 75 km in the time period between 10:28 and 11:35 UTC. This time period includes a descent from approximately 2100 m down to below cloud level (10:29 to 10:35 UTC), a leg at cloud base (10:35 to 10:52 UTC), an ascent through cloud with subsequent drying away of the ice collected inside cloud, and finally a leg at cloud top (11:07 to 11:35 UTC). With respect to the aerosol particle measurements, the time period 10:52 to 11:07 UTC, i.e., the ascent through cloud and the subsequent drying away of ice, is excluded from further analysis, as erroneous measurements due to icing of the aerosol inlet and/or droplet shattering (Weber et al., 1998) cannot be ruled out. The MPSS data from this period are grayed out in Fig. 10b, c.

The PNSDs at cloud top and at cloud base featured enhanced number concentrations in the nucleation mode size range from 10 nm to 20 nm, regardless of the cloud cover being closed or broken (Fig. 10). In contrast, in the PNSD measured during the descent towards cloud level around 10:30 UTC, which we assume to be representative for the free troposphere, concentrations in the sub-20 nm size range were low. This PNSD should be considered semi-quantitative only, as it represents an average over an altitude range of more than 1000 m. The presence/absence of particles in the size range from 10 nm to 20 nm is also clearly visible in Fig. 10c, with particles in the size range below 20 nm contributing approximately 65 %, 59 %, and 9 % to the total aerosol particle number concentrations at cloud top, cloud base, and in the free troposphere, respectively. A more detailed comparison between PNSDs measured at cloud top and at cloud base (Fig. 11) reveals an interesting effect. The overall shapes of the distributions are qualitatively similar, with the cloud top and cloud base accumulation mode concentrations following each other rather closely, while the number of Aitken and nucleation mode particles is reduced by roughly a factor of two to three at cloud base, resulting in a more pronounced Hoppel-minimum for the PNSDs measured at cloud base. Even a small shift of the accumulation mode at cloud base to larger sizes can be seen, which could be due to particle growth inside cloud.

https://doi.org/10.5194/egusphere-2026-2215
Preprint. Discussion started: 12 May 2026

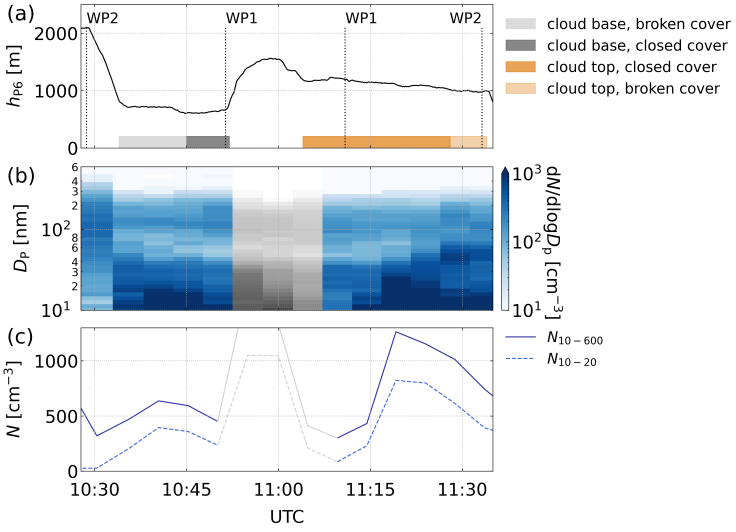

Figure 10. **(a)** P6 altitude during RF08 on 24 April 2024. **(b)** MPSS-measured PNSD. **(c)** Integral particle number concentrations in the total measured size range ($10\ \mathrm{nm} \leq D_\mathrm{p} \leq 600\ \mathrm{nm}$, solid line) and in the nucleation mode size range ($10\ \mathrm{nm} \leq D_\mathrm{p} \leq 20\ \mathrm{nm}$, dashed line), respectively. The data measured from 10:52 to 11:07 UTC are grayed out in panels (b) and (c) since erroneous measurements due to icing of the aerosol inlet and/or droplet shattering cannot be ruled out.

However, differences are too small to draw quantitative conclusions. To indicate the absence of nucleation mode particles in the free troposphere, also shown in Fig. 11 is the PNSD measured during the descent from 2100 m towards cloud level.

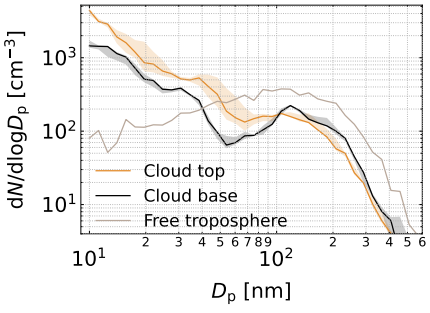

Figure 11. Median PNSDs measured at cloud top, cloud base, and in the free troposphere. The shaded areas represent the interquartile ranges.

Cloud tops, due to the prevailing high humidities and high actinic fluxes, which enhance photochemically driven processes, as well as the presence of potential particle precursors released from evaporating droplets, have been reported to be favorable locations for NPF to take place (e.g., Hegg et al., 1990; Clarke et al., 1998; Weber et al., 2001; Keil and Wendisch, 2001; Wehner et al., 2015). Overall, this leads us to the hypothesis that NPF in the vicinity of the cloud top led to the observed elevated concentrations of newly formed particles at cloud top and cloud base, with the newly formed particles being simultaneously mixed down and cloud processed (wet scavenging and/or growth depending on their size). Such a process is conceivable for

https://doi.org/10.5194/egusphere-2026-2215
Preprint. Discussion started: 12 May 2026

a marine ABL with the dynamics of radiatively cooled clouds (radiative cooling rate at cloud top $\approx -120\ \mathrm{K\,d^{-1}}$, Fig. S11, Lonardi et al. (2024)) and the related transport and mixing processes (Wood, 2012). In the Arctic, enhanced concentrations of particles in the size range from 20 nm to 300 nm at the top of stratus clouds were previously observed by Garrett et al. (2002), who suggested that recent particle formation at cloud top lead to these high concentrations.

Backward trajectory analysis of all air masses featuring newly formed particles in the vicinity of clouds

Fig.12 presents the results of the backward trajectory analysis carried out for all PNSD measurements featuring newly formed particles in the vicinity of clouds, which were observed during three different research flights on 23, 24 (case study), and 26 April.

Predominantly, the air masses approached from lower latitudes and moved northward, mainly in the last 48 hours prior to arrival (Fig. 12a). The trajectories traveled over the open sea in the last 18 to 60 hours and 90 to 100 hours (Fig. 12b), whereby they became warmer and picked up humidity (Fig. 12e-g). Since the moist air masses moved poleward, an increase of IVT_{north} is visible in the last 48 hours before arrival (Fig. 12h). Almost 75 % of the trajectories were in contact with the ABL during the last five days (Fig. 12i), presenting the opportunity for moisture and gaseous precursor uptake, potentially from the open ocean. In 89 % of the air masses, clouds had formed within the previous five days (Fig. 12i). The gradual decrease in potential temperature found in the last 24 hours prior to arrival (Fig. 12d) may result from the presence of these clouds, i.e., from cloud top radiative cooling.

Despite these similarities between the air mass histories, it is difficult to draw conclusions concerning the potential role of long-range transport in the observed events from the data available. Nevertheless, in our view, our measurement data clearly suggest that NPF in the vicinity of clouds was observed, with the region near clouds providing a favorable environment for NPF to take place. Considering the abundance of Arctic stratiform mixed-phase clouds (e.g., Shupe et al., 2013), NPF in the vicinity of such clouds may play an important role in the Arctic aerosol particle and CCN budgets.

4 Conclusions

In this study, we discussed the frequent occurrence of newly formed aerosol particles in the Arctic troposphere as observed during an airborne measurement campaign utilizing the Polar 6 research aircraft, which was conducted from 5 April 2024 to 2 May 2024. The Polar 6 was instrumented with dedicated meteorological and aerosol instrumentation collecting data over and around the Svalbard Archipelago, over the Fram Strait, and in the vicinity of Villum Research Station (Station Nord) in Greenland. We observed newly formed particles during all eleven research flights at various locations (approximately between 76°N to 85°N and 15°W to 26°E). Newly formed particles were encountered in an altitude range from about 60 m to 3900 m above sea level, i.e., throughout the flight altitude range covered by our aircraft. Specifically, these particles were detected in the free troposphere, inside the atmospheric boundary layer (ABL) over sea ice, and in the vicinity of clouds. No clear indications for

https://doi.org/10.5194/egusphere-2026-2215
Preprint. Discussion started: 12 May 2026

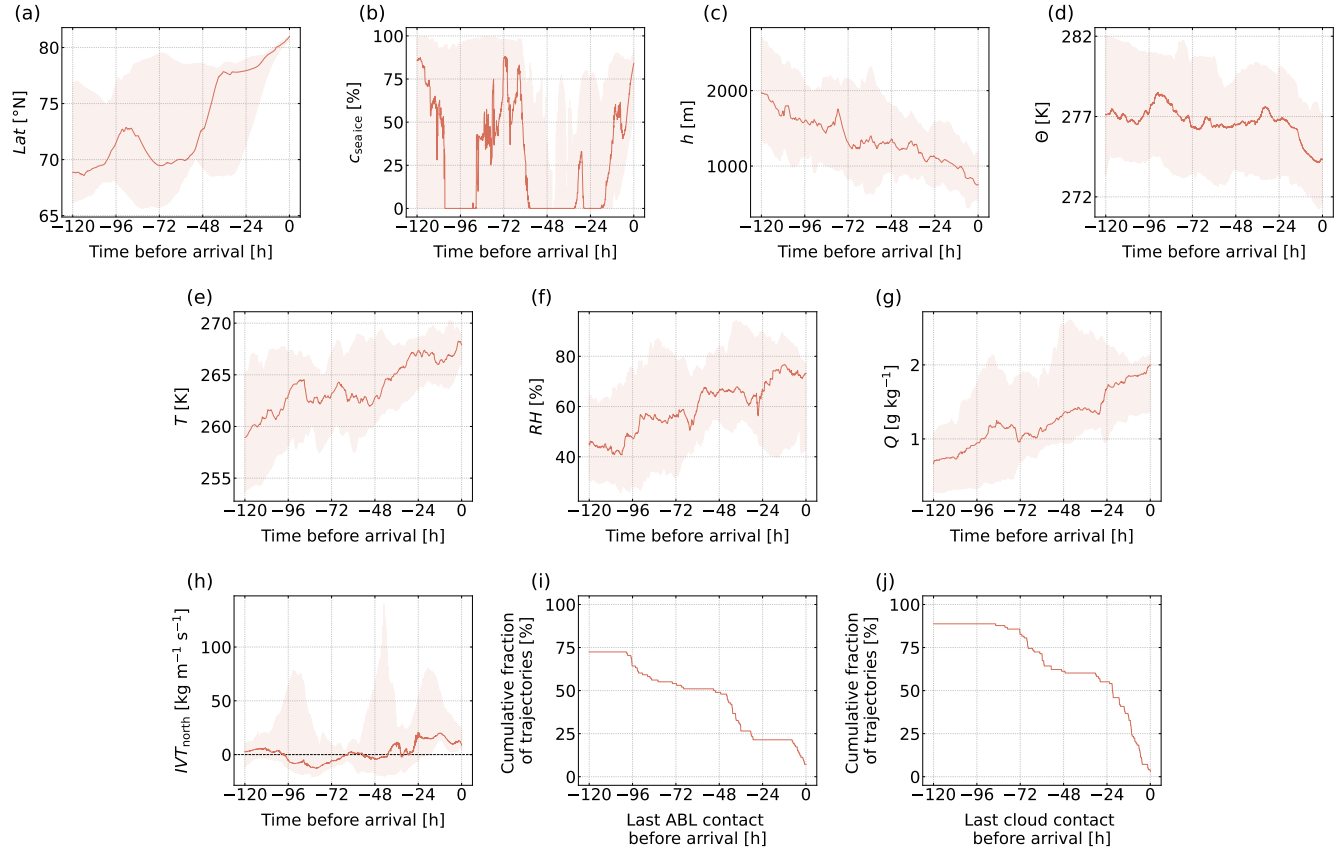

Figure 12. Meteorological parameters along backward trajectories linked to for newly formed particles detected in the vicinity of clouds. Shown, as a function of time prior to arrival, are median values (solid lines) and interquartile ranges (shaded areas) of **(a)** latitude Lat, **(b)** sea ice concentration c_{seaice}, **(c)** altitude h, **(d)** potential temperature Θ, **(e)** absolute temperature T, **(f)** relative humidity RH, **(g)** specific humidity Q, and **(h)** northward integrated water vapor transport IVT_{north}. The last two subplots show the cumulative fraction of the last contact of the trajectories with the **(i)** ABL and **(j)** clouds. Note that if the cumulative fraction does not increase to 100 % at $t = -120\,\mathrm{h}$, this indicates that a fraction of the trajectories was not in contact with the ABL/clouds during the last five days (the maximum time span the calculated trajectories cover).

newly formed particles inside the ABL over open ocean were found.

Newly formed particles in the free troposphere were encountered across large geographical areas and at different altitudes. Our respective analyses suggest a possibly important role of meridional transport in combination with cloud processing in Arctic free tropospheric new particle formation (NPF) as, e.g., warm-air intrusions may deliver the precursor gases to atmospheric conditions (high altitudes, intense solar radiation, low temperatures) favorable for NPF. With respect to the newly formed particles detected inside the ABL over sea ice, we conclude that these particles are presumably the result of regional NPF events induced by precursor gases (conceivably iodine components) originating from the sea ice, leads, or snow present in

https://doi.org/10.5194/egusphere-2026-2215
Preprint. Discussion started: 12 May 2026

the measurement region. However, contributions of higher-latitude Arctic (precursor) sources cannot be ruled out. Concerning newly formed particles observed at both cloud tops and cloud bases, we found clear indications that these particles are very likely formed at the cloud tops and subsequently mixed down to the cloud bases, with the cloud tops providing a favorable environment for NPF to occur.

Taken together, our results show that newly formed particles were frequently present and very likely produced in the both the Arctic free troposphere and the Arctic ABL during our measurements in spring 2024, while prior observations predominantly suggested that NPF inside the ABL is the most common source of secondary aerosol particles in the Arctic. In particular, for the first time, our study presents observational results which indicate that NPF in the Arctic free troposphere could be a geographically widespread phenomenon, and that free tropospheric NPF is connected to warm-air intrusions. This transport pathway of precursor gases and/or newly formed particles from lower latitudes to the Arctic free troposphere was previously suggested in a modeling study by Price et al. (2023), but to date had not been substantiated by analysis of in situ-measured data. We present observational evidence which supports the findings of Price et al. (2023) and emphasizes the importance of free tropospheric sources of newly formed particles.

Further modeling studies are required to assess the impact of newly formed particles occurring over large geographical areas and a wide range of altitudes inside and above the Arctic ABL on the Arctic aerosol and cloud condensation nuclei (CCN) budgets, and ultimately on the Arctic climate. In particular, because relatively small, sub-100 nm particles readily act as CCN in the clean Arctic atmosphere, the geographically-extended, frequent occurrence of newly formed particles might exert an important influence on Arctic aerosol-cloud-climate interactions. Future observational campaigns would profit from trace gas measurements and fast, size-resolved measurements of particles with diameters of less than 10 nm, e.g., with multiple condensation particle counters featuring different lower cut-off diameters. Such measurements would facilitate the identification of the relevant precursor gases and the precise nucleation region. Importantly, prospective studies should include vertical measurements and target both the Arctic ABL and free troposphere.

Finally, in a rapidly warming Arctic, where the sea ice continues to retreat, more clouds might be present in the future, and the occurrence of warm-air intrusions is expected to increase, NPF frequency and location will likely be affected by these changes. Especially NPF in the free troposphere, linked to warm-air intrusions, and at the tops of Arctic stratiform clouds, might significantly impact current and future Arctic aerosol and CCN budgets due to its potentially large geographical extent and frequent occurrence, and should therefore be considered in atmospheric models for the prediction of future Arctic weather and climate.

Data availability. Master tracks are available on PANGAEA for all research flights of the BACSAM II campaign (Jurányi et al., 2024). Backward trajectory data are available on PANGAEA for all research flights of the BACSAM II campaign (Kirbus and Wendisch, 2024). PNSD data from all research flights of the BACSAM II campaign were published on PANGAEA on 14 April 2026 (Simon et al., 2026). A DOI will be registered within 28 days following the publication. Sea ice data were retrieved from www.seaice.uni-bremen.de (Spreen et al., 2008). MODIS-TERRA satellite images were retrieved from https://wvs.earthdata.nasa.gov.

https://doi.org/10.5194/egusphere-2026-2215
Preprint. Discussion started: 12 May 2026

Author contributions. DJS participated in the data collection and flight planning during the BACSAM II campaign, analyzed and interpreted the data, and wrote the manuscript. JS participated in the data collection and flight planning, discussed the data, and contributed to the writing. JH participated in the data collection and flight planning, and processed the position, nose boom, and humidity data. BK performed the trajectory calculations and supported their analysis. JM participated in the data collection, flight planning, and calculated the radiative heating/cooling rates. MH, BW, LK,AMJ, and MW participated in the flight planning, and the data collection and related discussions. KW was responsible for the development of the MPSS system. AH and ZJ functioned as PIs during the campaign. AH, ZJ, SH, GCR, MW, and MLP contributed to the discussion of the results. FS conceived the study, functioned as PI during the campaign, and contributed to data interpretation and writing. All authors read and edited the manuscript.

Competing interests. The authors declare no competing interests.

Acknowledgements. We gratefully acknowledge the funding by the Deutsche Forschungsgemeinschaft (DFG, German Research Foundation) – Project Number 268020496 – TRR 172, within the framework of the Transregional Collaborative Research Center "ArctiC Amplification: Climate Relevant Atmospheric and SurfaCe Processes, and Feedback Mechanisms (AC)^3", as well as the support of the Alfred-Wegener-Institute, Helmholtz Centre for Polar and Marine Research through grant number AWI_PA_02172. The authors used a large language model (ChatGPT by OpenAI) solely to support coding tasks; all scientific reasoning, methodological decisions, analyses, and conclusions were developed independently by the authors.

https://doi.org/10.5194/egusphere-2026-2215
Preprint. Discussion started: 12 May 2026

References

Allan, J. D., Williams, P. I., Najera, J., Whitehead, J. D., Flynn, M. J., Taylor, J. W., Liu, D., Darbyshire, E., Carpenter, L. J., Chance, R., Andrews, S. J., Hackenberg, S. C., and McFiggans, G.: Iodine observed in new particle formation events in the Arctic atmosphere during ACCACIA, Atmospheric Chemistry and Physics, 15, 5599–5609, https://doi.org/10.5194/acp-15-5599-2015, 2015.

Andreae, M. and Rosenfeld, D.: Aerosol–cloud–precipitation interactions. Part 1. The nature and sources of cloud-active aerosols, Earth-Science Reviews, 89, 13–41, https://doi.org/10.1016/j.earscirev.2008.03.001, 2008.

Asmi, E., Kondratyev, V., Brus, D., Laurila, T., Lihavainen, H., Backman, J., Vakkari, V., Aurela, M., Hatakka, J., Viisanen, Y., Uttal, T., Ivakhov, V., and Makshtas, A.: Aerosol size distribution seasonal characteristics measured in Tiksi, Russian Arctic, Atmospheric Chemistry and Physics, 16, 1271–1287, https://doi.org/10.5194/acp-16-1271-2016, 2016.

Atkinson, H. M., Huang, R.-J., Chance, R., Roscoe, H. K., Hughes, C., Davison, B., Schönhardt, A., Mahajan, A. S., Saiz-Lopez, A., Hoffmann, T., and Liss, P. S.: Iodine emissions from the sea ice of the Weddell Sea, Atmospheric Chemistry and Physics, 12, 11 229–11 244, https://doi.org/10.5194/acp-12-11229-2012, 2012.

Baccarini, A., Karlsson, L., Dommen, J., Duplessis, P., Vüllers, J., Brooks, I. M., Saiz-Lopez, A., Salter, M., Tjernström, M., Baltensperger, U., et al.: Frequent new particle formation over the high Arctic pack ice by enhanced iodine emissions, Nature Communications, 11, 4924, https://doi.org/10.1038/s41467-020-18551-0, 2020.

Beck, L. J., Sarnela, N., Junninen, H., Hoppe, C. J., Garmash, O., Bianchi, F., Riva, M., Rose, C., Peräkylä, O., Wimmer, D., et al.: Differing mechanisms of new particle formation at two Arctic sites, Geophysical Research Letters, 48, e2020GL091 334, https://doi.org/10.1029/2020GL091334, 2021.

Bintanja, R., van der Wiel, K., van der Linden, E. C., Reusen, J., Bogerd, L., Krikken, F., and Selten, F. M.: Strong future increases in Arctic precipitation variability linked to poleward moisture transport, Science Advances, 6, eaax6869, https://doi.org/10.1126/sciadv.aax6869, 2020.

Box, J. E., Colgan, W. T., Christensen, T. R., Schmidt, N. M., Lund, M., Parmentier, F.-J. W., Brown, R., Bhatt, U. S., Euskirchen, E. S., Romanovsky, V. E., Walsh, J. E., Overland, J. E., Wang, M., Corell, R. W., Meier, W. N., Wouters, B., Mernild, S., Mård, J., Pawlak, J., and Olsen, M. S.: Key indicators of Arctic climate change: 1971–2017, Environmental Research Letters, 14, 045 010, https://doi.org/10.1088/1748-9326/aafc1b, 2019.

Burkart, J., Willis, M. D., Bozem, H., Thomas, J. L., Law, K., Hoor, P., Aliabadi, A. A., Köllner, F., Schneider, J., Herber, A., et al.: Summertime observations of elevated levels of ultrafine particles in the high Arctic marine boundary layer, Atmospheric Chemistry and Physics, 17, 5515–5535, https://doi.org/10.5194/acp-17-5515-2017, 2017.

Carslaw, K., Lee, L., Reddington, C., Pringle, K., Rap, A., Forster, P., Mann, G., Spracklen, D., Woodhouse, M., Regayre, L., et al.: Large contribution of natural aerosols to uncertainty in indirect forcing, Nature, 503, 67–71, https://doi.org/10.1038/nature12674, 2013.

Clarke, A., Varner, J., Eisele, F., Mauldin, R., Tanner, D., and Litchy, M.: Particle production in the remote marine atmosphere: Cloud outflow and subsidence during ACE 1, Journal of Geophysical Research: Atmospheres, 103, 16 397–16 409, https://doi.org/10.1029/97JD02987, 1998.

Croft, B., Wentworth, G. R., Martin, R. V., Leaitch, W. R., Murphy, J. G., Murphy, B. N., Kodros, J. K., Abbatt, J. P., and Pierce, J. R.: Contribution of Arctic seabird-colony ammonia to atmospheric particles and cloud-albedo radiative effect, Nature Communications, 7, 13 444, https://doi.org/10.1038/ncomms13444, 2016.

https://doi.org/10.5194/egusphere-2026-2215
Preprint. Discussion started: 12 May 2026

Cuevas, C. A., Maffezzoli, N., Corella, J. P., Spolaor, A., Vallelonga, P., Kjær, H. A., Simonsen, M., Winstrup, M., Vinther, B., Horvat, C., et al.: Rapid increase in atmospheric iodine levels in the North Atlantic since the mid-20th century, Nature Communications, 9, 1452, https://doi.org/https://doi.org/10.1038/s41467-018-03756-1, 2018.

Dada, L., Angot, H., Beck, I., Baccarini, A., Quéléver, L. L., Boyer, M., Laurila, T., Brasseur, Z., Jozef, G., De Boer, G., et al.: A central arctic extreme aerosol event triggered by a warm air-mass intrusion, Nature Communications, 13, 5290, https://doi.org/10.1038/s41467-022-32872-2, 2022.

Dall'Osto, M., Beddows, D., Tunved, P., Krejci, R., Ström, J., Hansson, H.-C., Yoon, Y., Park, K.-T., Becagli, S., Udisti, R., et al.: Arctic sea ice melt leads to atmospheric new particle formation, Scientific Reports, 7, 3318, https://doi.org/10.1038/s41598-017-03328-1, 2017.

Dall'Osto, M., Geels, C., Beddows, D., Boertmann, D., Lange, R., Nøjgaard, J., Harrison, R. M., Simo, R., Skov, H., and Massling, A.: Regions of open water and melting sea ice drive new particle formation in North East Greenland, Scientific Reports, 8, 6109, https://doi.org/10.1038/s41598-018-24426-8, 2018.

Dall'Osto, M., Park, J., Kim, J.-H., Kang, S.-H., Park, K., Beddows, D., Harrison, R. M., and Yoon, Y. J.: Arctic ship-based evidence of new particle formation events in the Chukchi and East Siberian Seas, Atmospheric Environment, 223, 117 232, https://doi.org/10.1016/j.atmosenv.2019.117232, 2020.

Engvall, A.-C., Krejci, R., Ström, J., Minikin, A., Treffeisen, R., Stohl, A., and Herber, A.: In-situ airborne observations of the microphysical properties of the Arctic tropospheric aerosol during late spring and summer, Tellus B: Chemical and Physical Meteorology, 60, 392–404, https://doi.org/10.1111/j.1600-0889.2008.00348.x, 2008.

Forster, P., Storelvmo, T., Armour, K., Collins, W., Dufresne, J.-L., Frame, D., Lunt, D. J., Mauritsen, T., Palmer, M. D., Watanabe, M., Wild, M., and Zhang, H.: The Earth's Energy Budget, Climate Feedbacks, and Climate Sensitivity, in: Climate Change 2021: The Physical Science Basis. Contribution of Working Group I to the Sixth Assessment Report of the Intergovernmental Panel on Climate Change, edited by Masson-Delmotte, V., Zhai, P., Pirani, A., Connors, S. L., Péan, C., Berger, S., Caud, N., Chen, Y., Goldfarb, L., Gomis, M. I., Huang, M., Leitzell, K., Lonnoy, E., Matthews, J. B. R., Maycock, T. K., Waterfield, T., Yelekçi, O., Yu, R., and Zhou, B., pp. 923–1054, Cambridge University Press, Cambridge, United Kingdom and New York, NY, USA, https://doi.org/10.1017/9781009157896.009, 2021.

Freud, E., Krejci, R., Tunved, P., Leaitch, R., Nguyen, Q. T., Massling, A., Skov, H., and Barrie, L.: Pan-Arctic aerosol number size distributions: seasonality and transport patterns, Atmospheric Chemistry and Physics, 17, 8101–8128, https://doi.org/10.5194/acp-17-8101-2017, 2017.

Galí, M., Devred, E., Babin, M., and Levasseur, M.: Decadal increase in Arctic dimethylsulfide emission, Proceedings of the National Academy of Sciences, 116, 19 311–19 317, https://doi.org/10.1073/pnas.190437811, 2019.

Gálvez, O., Baeza-Romero, M. T., Sanz, M., and Saiz-Lopez, A.: Photolysis of frozen iodate salts as a source of active iodine in the polar environment, Atmospheric Chemistry and Physics, 16, 12 703–12 713, https://doi.org/10.5194/acp-16-12703-2016, 2016.

Garrett, T. J., Hobbs, P. V., and Radke, L. F.: High Aitken nucleus concentrations above cloud tops in the Arctic, Journal of the Atmospheric Sciences, 59, 779–783, https://doi.org/10.1175/1520-0469(2001)059<0779:HANCAC>2.0.CO;2, 2002.

Gordon, H., Kirkby, J., Baltensperger, U., Bianchi, F., Breitenlechner, M., Curtius, J., Dias, A., Dommen, J., Donahue, N. M., Dunne, E. M., et al.: Causes and importance of new particle formation in the present-day and preindustrial atmospheres, Journal of Geophysical Research: Atmospheres, 122, 8739–8760, https://doi.org/10.1002/2017JD026844, 2017.

Hartmann, J., Gehrmann, M., Kohnert, K., Metzger, S., and Sachs, T.: New calibration procedures for airborne turbulence measurements and accuracy of the methane fluxes during the AirMeth campaigns, Atmospheric Measurement Techniques, 11, 4567–4581, https://doi.org/10.5194/amt-11-4567-2018, 2018.

https://doi.org/10.5194/egusphere-2026-2215
Preprint. Discussion started: 12 May 2026

Hegg, D. A., Radke, L. F., and Hobbs, P. V.: Particle production associated with marine clouds, Journal of Geophysical Research: Atmospheres, 95, 13 917–13 926, https://doi.org/10.1029/JD095iD09p13917, 1990.

Hersbach, H., Bell, B., Berrisford, P., Hirahara, S., Horányi, A., Muñoz-Sabater, J., Nicolas, J., Peubey, C., Radu, R., Schepers, D., et al.: The ERA5 global reanalysis, Quarterly Journal of the Royal Meteorological Society, 146, 1999–2049, https://doi.org/10.1002/qj.3803, 2020.

Hill, V. L. and Manley, S. L.: Release of reactive bromine and iodine from diatoms and its possible role in halogen transfer in polar and tropical oceans, Limnology and Oceanography, 54, 812–822, https://doi.org/10.4319/lo.2009.54.3.0812, 2009.

Jurányi, Z., Stratmann, F., Herber, A., Wendisch, M., and Borrmann, S.: Master tracks in different resolutions during POLAR 6 campaign P6-247_BACSAM2_2024, https://doi.org/10.1594/PANGAEA.971763, 2024.

Jurányi, Z., Lüpkes, C., Stratmann, F., Hartmann, J., Schaefer, J., Jörss, A.-M., Schulz, A., Wetzel, B., Simon, D., Gebhard, E., Stöhr, M., Hofmann, P., Kalmbach, D., Grawe, S., Wendisch, M., and Herber, A.: The T-Bird – a new aircraft-towed instrument platform to measure aerosol properties and turbulence close to the surface: introduction to the aerosol measurement system, Atmospheric Measurement Techniques, 18, 3477–3494, https://doi.org/10.5194/amt-18-3477-2025, 2025.

Keil, A. and Wendisch, M.: Bursts of Aitken mode and ultrafine particles observed at the top of continental boundary layer clouds, Journal of Aerosol Science, 32, 649–660, https://doi.org/10.1016/S0021-8502(00)00102-6, 2001.

Kerminen, V.-M., Chen, X., Vakkari, V., Petäjä, T., Kulmala, M., and Bianchi, F.: Atmospheric new particle formation and growth: review of field observations, Environmental Research Letters, 13, 103 003, https://doi.org/10.1088/1748-9326/aadf3c, 2018.

Kim, K., Yabushita, A., Okumura, M., Saiz-Lopez, A., Cuevas, C. A., Blaszczak-Boxe, C. S., Min, D. W., Yoon, H.-I., and Choi, W.: Production of molecular iodine and tri-iodide in the frozen solution of iodide: implication for polar atmosphere, Environmental Science & Technology, 50, 1280–1287, https://doi.org/10.1021/acs.est.5b05148, 2016.

Kirbus, B. and Wendisch, M.: Five-day backwards trajectories at one minute resolution along the flight tracks of the Polar 6 research aircraft during BACSAM II, https://doi.org/10.1594/PANGAEA.971694, 2024.

Kulmala, M. and Kerminen, V.-M.: On the formation and growth of atmospheric nanoparticles, Atmospheric Research, 90, 132–150, https://doi.org/10.1016/j.atmosres.2008.01.005, 2008.

Kulmala, M., Vehkamäki, H., Petäjä, T., Dal Maso, M., Lauri, A., Kerminen, V.-M., Birmili, W., and McMurry, P.: Formation and growth rates of ultrafine atmospheric particles: a review of observations, Journal of Aerosol Science, 35, 143–176, https://doi.org/10.1016/j.jaerosci.2003.10.003, 2004.

Kupiszewski, P., Leck, C., Tjernström, M., Sjogren, S., Sedlar, J., Graus, M., Müller, M., Brooks, B., Swietlicki, E., Norris, S., et al.: Vertical profiling of aerosol particles and trace gases over the central Arctic Ocean during summer, Atmospheric Chemistry and Physics, 13, 12 405–12 431, https://doi.org/10.5194/acp-13-12405-2013, 2013.

Leaitch, W. R., Sharma, S., Huang, L., Toom-Sauntry, D., Chivulescu, A., Macdonald, A. M., von Salzen, K., Pierce, J. R., Bertram, A. K., Schroder, J. C., et al.: Dimethyl sulfide control of the clean summertime Arctic aerosol and cloud, Elementa, 1, 000 017, https://doi.org/doi.org/10.12952/journal.elementa.000017, 2013.

Lee, S.-H., Gordon, H., Yu, H., Lehtipalo, K., Haley, R., Li, Y., and Zhang, R.: New particle formation in the atmosphere: From molecular clusters to global climate, Journal of Geophysical Research: Atmospheres, 124, 7098–7146, https://doi.org/10.1029/2018JD029356, 2019.

Lonardi, M., Akansu, E. F., Ehrlich, A., Mazzola, M., Pilz, C., Shupe, M. D., Siebert, H., and Wendisch, M.: Tethered balloon-borne observations of thermal-infrared irradiance and cooling rate profiles in the Arctic atmospheric boundary layer, Atmospheric Chemistry and Physics, 24, 1961–1978, https://doi.org/10.5194/acp-24-1961-2024, 2024.

https://doi.org/10.5194/egusphere-2026-2215
Preprint. Discussion started: 12 May 2026

Mauritsen, T., Sedlar, J., Tjernström, M., Leck, C., Martin, M., Shupe, M., Sjogren, S., Sierau, B., Persson, P. O. G., Brooks, I. M., and Swietlicki, E.: An Arctic CCN-limited cloud-aerosol regime, Atmospheric Chemistry and Physics, 11, 165–173, https://doi.org/10.5194/acp-11-165-2011, 2011.

Merikanto, J., Spracklen, D., Mann, G., Pickering, S., and Carslaw, K.: Impact of nucleation on global CCN, Atmospheric Chemistry and Physics, 9, 8601–8616, https://doi.org/10.5194/acp-9-8601-2009, 2009.

Perry, K. D. and Hobbs, P. V.: Further evidence for particle nucleation in clear air adjacent to marine cumulus clouds, Journal of Geophysical Research: Atmospheres, 99, 22 803–22 818, https://doi.org/10.1029/94JD01926, 1994.

Pierce, J. and Adams, P.: Uncertainty in global CCN concentrations from uncertain aerosol nucleation and primary emission rates, Atmospheric Chemistry and Physics, 9, 1339–1356, https://doi.org/10.5194/acp-9-1339-2009., 2009.

Pilz, C., Cassano, J. J., de Boer, G., Kirbus, B., Lonardi, M., Pöhlker, M., Shupe, M. D., Siebert, H., Wendisch, M., and Wehner, B.: Tethered balloon measurements reveal enhanced aerosol occurrence aloft interacting with Arctic low-level clouds, Elementa: Science of the Anthropocene, 12, https://doi.org/10.1525/elementa.2023.00120, 2024.

Price, R., Baccarini, A., Schmale, J., Zieger, P., Brooks, I. M., Field, P., and Carslaw, K. S.: Late summer transition from a free-tropospheric to boundary layer source of Aitken mode aerosol in the high Arctic, Atmospheric Chemistry and Physics, 23, 2927–2961, https://doi.org/10.5194/acp-23-2927-2023, 2023.

Raso, A. R. W., Custard, K. D., May, N. W., Tanner, D., Newburn, M. K., Walker, L., Moore, R. J., Huey, L. G., Alexander, L., Shepson, P. B., and Pratt, K. A.: Active molecular iodine photochemistry in the Arctic, Proceedings of the National Academy of Sciences, 114, 10 053–10 058, https://doi.org/10.1073/pnas.1702803114, 2017.

Schmale, J. and Baccarini, A.: Progress in unraveling atmospheric new particle formation and growth across the Arctic, Geophysical Research Letters, 48, e2021GL094 198, https://doi.org/10.1029/2021GL094198, 2021.

Schmale, J., Zieger, P., and Ekman, A. M.: Aerosols in current and future Arctic climate, Nature Climate Change, 11, 95–105, https://doi.org/10.1038/s41558-020-00969-5, 2021.

Seinfeld, J. H. and Pandis, S. N.: Atmospheric chemistry and physics: from air pollution to climate change, John Wiley & Sons, 2006.

Serreze, M. C. and Barry, R. G.: Processes and impacts of Arctic amplification: A research synthesis, Global and Planetary Change, 77, 85–96, https://doi.org/10.1016/j.gloplacha.2011.03.004, 2011.

Serreze, M. C. and Francis, J. A.: The Arctic amplification debate, Climatic Change, 76, 241–264, https://doi.org/10.1007/s10584-005-9017-y, 2006.

Shupe, M., Persson, P., Brooks, I., Tjernström, M., Sedlar, J., Mauritsen, T., Sjogren, S., and Leck, C.: Cloud and boundary layer interactions over the Arctic sea ice in late summer, Atmospheric Chemistry and Physics, 13, 9379–9399, https://doi.org/10.5194/acp-13-9379-2013, 2013.

Simon, D. J., Schaefer, J., Hartmann, M., Weinhold, K., and Stratmann, F.: Airborne in-situ measurements of aerosol particle number size distributions during the BACSAM II campaign in April 2024, https://doi.pangaea.de/10.1594/PANGAEA.993546, 2026.

Sipilä, M., Sarnela, N., Jokinen, T., Henschel, H., Junninen, H., Kontkanen, J., Richters, S., Kangasluoma, J., Franchin, A., Peräkylä, O., et al.: Molecular-scale evidence of aerosol particle formation via sequential addition of HIO3, Nature, 537, 532–534, https://doi.org/10.1038/nature19314, 2016.

Spreen, G., Kaleschke, L., and Heygster, G.: Sea ice remote sensing using AMSR-E 89-GHz channels, Journal of Geophysical Research: Oceans, 113, https://doi.org/10.1029/2005JC003384, 2008.

https://doi.org/10.5194/egusphere-2026-2215
Preprint. Discussion started: 12 May 2026

Sprenger, M. and Wernli, H.: The LAGRANTO Lagrangian analysis tool – version 2.0, Geoscientific Model Development, 8, 2569–2586, https://doi.org/10.5194/gmd-8-2569-2015, 2015.

Stroeve, J., Holland, M. M., Meier, W., Scambos, T., and Serreze, M.: Arctic sea ice decline: Faster than forecast, Geophysical research letters, 34, https://doi.org/10.1029/2007GL029703, 2007.

Ström, J., Engvall, A. C., Delbart, F., Krejci, R., and Treffeisen, R.: On small particles in the Arctic summer boundary layer: observations at two different heights near Ny-Ålesund, Svalbard, Tellus B: Chemical and Physical Meteorology, 61, 473–482, https://doi.org/10.1111/j.1600-0889.2008.00412.x, 2009.

Weber, R., Clarke, A., Litchy, M., Li, J., Kok, G., Schillawski, R., and McMurry, P.: Spurious aerosol measurements when sampling from aircraft in the vicinity of clouds, Journal of Geophysical Research: Atmospheres, 103, 28 337–28 346, https://doi.org/10.1029/98JD02086, 1998.

Weber, R., Chen, G., Davis, D., Mauldin III, R., Tanner, D., Eisele, F., Clarke, A., Thornton, D., and Bandy, A.: Measurements of enhanced H_2SO_4 and 3–4 nm particles near a frontal cloud during the First Aerosol Characterization Experiment (ACE 1), Journal of Geophysical Research: Atmospheres, 106, 24 107–24 117, https://doi.org/10.1029/2000JD000109, 2001.

Weber, R., Orsini, D., Wang, B., Scheuer, E., Talbot, R., Dibb, J. E., Seid, G., DeBell, L., Mauldin, R., Kosciuch, E., et al.: Investigations into free tropospheric new particle formation in the central Canadian arctic during the winter/spring transition as part of TOPSE, Journal of Geophysical Research: Atmospheres, 108, https://doi.org/10.1029/2002JD002239, 2003.

Wehner, B., Werner, F., Ditas, F., Shaw, R. A., Kulmala, M., and Siebert, H.: Observations of new particle formation in enhanced UV irradiance zones near cumulus clouds, Atmospheric Chemistry and Physics, 15, 11 701–11 711, https://doi.org/10.5194/acp-15-11701-2015, 2015.

Wendisch, M., Brückner, M., Burrows, J., Crewell, S., Dethloff, K., Ebell, K., Lüpkes, C., Macke, A., Notholt, J., Quaas, J., et al.: Understanding causes and effects of rapid warming in the Arctic, Eos, https://doi.org/10.1029/2017EO064803, 2017.

Wendisch, M., Brückner, M., Crewell, S., Ehrlich, A., Notholt, J., Lüpkes, C., Macke, A., Burrows, J., Rinke, A., Quaas, J., et al.: Atmospheric and surface processes, and feedback mechanisms determining Arctic amplification: A review of first results and prospects of the $(\mathcal{AC})^3$ project, Bulletin of the American Meteorological Society, 104, E208–E242, https://doi.org/10.1175/BAMS-D-21-0218.1, 2023.

Wendisch, M., Crewell, S., Ehrlich, A., Herber, A., Kirbus, B., Lüpkes, C., Mech, M., Abel, S. J., Akansu, E. F., Ament, F., Aubry, C., Becker, S., Borrmann, S., Bozem, H., Brückner, M., Clemen, H.-C., Dahlke, S., Dekoutsidis, G., Delanoë, J., De La Torre Castro, E., Dorff, H., Dupuy, R., Eppers, O., Ewald, F., George, G., Gorodetskaya, I. V., Grawe, S., Groß, S., Hartmann, J., Henning, S., Hirsch, L., Jäkel, E., Joppe, P., Jourdan, O., Jurányi, Z., Karalis, M., Kellermann, M., Klingebiel, M., Lonardi, M., Lucke, J., Luebke, A. E., Maahn, M., Maherndl, N., Maturilli, M., Mayer, B., Mayer, J., Mertes, S., Michaelis, J., Michalkov, M., Mioche, G., Moser, M., Müller, H., Neggers, R., Ori, D., Paul, D., Paulus, F. M., Pilz, C., Pithan, F., Pöhlker, M., Pörtge, V., Ringel, M., Risse, N., Roberts, G. C., Rosenburg, S., Röttenbacher, J., Rückert, J., Schäfer, M., Schaefer, J., Schemann, V., Schirmacher, I., Schmidt, J., Schmidt, S., Schneider, J., Schnitt, S., Schwarz, A., Siebert, H., Sodemann, H., Sperzel, T., Spreen, G., Stevens, B., Stratmann, F., Svensson, G., Tatzelt, C., Tuch, T., Vihma, T., Voigt, C., Volkmer, L., Walbröl, A., Weber, A., Wehner, B., Wetzel, B., Wirth, M., and Zinner, T.: Overview: quasi-Lagrangian observations of Arctic air mass transformations – introduction and initial results of the HALO–$(\mathcal{AC})^3$ aircraft campaign, Atmospheric Chemistry and Physics, 24, 8865–8892, https://doi.org/10.5194/acp-24-8865-2024, 2024.

Wendisch, M., Kirbus, B., Ori, D., Shupe, M. D., Crewell, S., Sodemann, H., and Schemann, V.: Observed and modeled Arctic air-mass transformations during warm air intrusions and cold air outbreaks, Atmospheric Chemistry and Physics, 25, 15 047–15 076, https://doi.org/10.5194/acp-25-15047-2025, 2025.

https://doi.org/10.5194/egusphere-2026-2215
Preprint. Discussion started: 12 May 2026

Wesche, C., Steinhage, D., and Nixdorf, U.: Polar aircraft Polar5 and Polar6 operated by the Alfred Wegener institute, Journal of Large-Scale Research Facilities, 2, A87–A87, https://doi.org/10.17815/jlsrf-2-153, 2016.

Wiedensohler, A., Covert, D. S., Swietlicki, E., Aalto, P., Heintzenberg, J., and Leck, C.: Occurrence of an ultrafine particle mode less than 20 nm in diameter in the marine boundary layer during Arctic summer and autumn, Tellus B, 48, 213–222, https://doi.org/10.3402/tellusb.v48i2.15887, 1996.

Wiedensohler, A., Birmili, W., Nowak, A., Sonntag, A., Weinhold, K., Merkel, M., Wehner, B., Tuch, T., Pfeifer, S., Fiebig, M., Fjäraa, A. M., Asmi, E., Sellegri, K., Depuy, R., Venzac, H., Villani, P., Laj, P., Aalto, P., Ogren, J. A., Swietlicki, E., Williams, P., Roldin, P., Quincey, P., Hüglin, C., Fierz-Schmidhauser, R., Gysel, M., Weingartner, E., Riccobono, F., Santos, S., Grüning, C., Faloon, K., Beddows, D., Harrison, R., Monahan, C., Jennings, S. G., O'Dowd, C. D., Marinoni, A., Horn, H.-G., Keck, L., Jiang, J., Scheckman, J., McMurry, P. H., Deng, Z., Zhao, C. S., Moerman, M., Henzing, B., de Leeuw, G., Löschau, G., and Bastian, S.: Mobility particle size spectrometers: harmonization of technical standards and data structure to facilitate high quality long-term observations of atmospheric particle number size distributions, Atmospheric Measurement Techniques, 5, 657–685, https://doi.org/10.5194/amt-5-657-2012, 2012.

Wiedensohler, A., Wiesner, A., Weinhold, K., Birmili, W., Hermann, M., Merkel, M., Müller, T., Pfeifer, S., Schmidt, A., Tuch, T., et al.: Mobility particle size spectrometers: Calibration procedures and measurement uncertainties, Aerosol Science and Technology, 52, 146–164, https://doi.org/10.1080/02786826.2017.1387229, 2018.

Willis, M. D., Burkart, J., Thomas, J. L., Köllner, F., Schneider, J., Bozem, H., Hoor, P. M., Aliabadi, A. A., Schulz, H., Herber, A. B., Leaitch, W. R., and Abbatt, J. P. D.: Growth of nucleation mode particles in the summertime Arctic: a case study, Atmospheric Chemistry and Physics, 16, 7663–7679, https://doi.org/10.5194/acp-16-7663-2016, 2016.

Willis, M. D., Köllner, F., Burkart, J., Bozem, H., Thomas, J. L., Schneider, J., Aliabadi, A. A., Hoor, P. M., Schulz, H., Herber, A. B., et al.: Evidence for marine biogenic influence on summertime Arctic aerosol, Geophysical Research Letters, 44, 6460–6470, https://doi.org/10.1002/2017GL073359, 2017.

Willis, M. D., Leaitch, W. R., and Abbatt, J. P.: Processes controlling the composition and abundance of Arctic aerosol, Reviews of Geophysics, 56, 621–671, https://doi.org/10.1029/2018RG000602, 2018.

Wood, R.: Stratocumulus clouds, Monthly Weather Review, 140, 2373–2423, https://doi.org/10.1175/MWR-D-11-00121.1, 2012.